

# Bio-based structurally compatible polymer blends based on lignin and thermoplastic elastomer polyurethane as carbon fiber precursors

*Mario Culebras<sup>a\*</sup>, Anne Beaucamp<sup>a</sup>, Yan Wang<sup>a</sup>, Manuel M. Clauss<sup>b</sup>, Erik Frank<sup>b</sup> and  
Maurice N. Collins<sup>a\*</sup>*

<sup>a</sup>Stokes Laboratories, Bernal Institute, University of Limerick, Limerick (Ireland)

<sup>b</sup> German Institutes for Textile and Fiber Research, Körschtalstrasse 26, 73770 Denkendorf  
(Germany)

Email: [mario.culebrasrubio@ul.ie](mailto:mario.culebrasrubio@ul.ie); [Maurice.collins@ul.ie](mailto:Maurice.collins@ul.ie)

**ABSTRACT:** The production of carbon fibers based on lignin reduces the cost and the environmental impact associated with carbon fiber manufacture. However, the melt processing of lignin as a carbon fiber precursor is challenging due to its brittleness and limited thermoplastic behavior. For this reason we produce biopolymer blends based on Alcell organosolv hardwood lignin, hydroxypropyl modified Kraft hardwood and a thermoplastic elastomer polyurethane (TPU). Samples with TPU content greater than 30 % showed excellent melt processability and carbonization yield (35 % carbon yield for the samples containing 30 % of TPU). The thermal properties were analyzed by differential scanning calorimetry, rheology and thermogravimetric analysis. Fourier infrared measurements were utilised to explain the lignin/TPU interactions which governed the thermal and rheological behaviour of the blends. SEM analysis showed that the blends produce a homogeneous structure which was void free after carbonization. These structurally complimentary biopolymeric blends should open up new avenues for lignin valorization and bring closer the realization of the production of carbon fibers from biosources.

**KEYWORDS:** Lignin, polyurethane, carbon fibers, thermal properties, biopolymers

## **Introduction**

Carbon fibers are one of the most valuable products in structural applications such as: aerospace, military, sports goods, automobile and energy. Currently, the vast majority of the carbon fibers are produced by heat treatment and pyrolysis of polyacrylonitrile (PAN) that is synthesized using petroleum sources.<sup>1-3</sup> There are several disadvantages associated with the use of PAN as carbon fiber precursor such as: high cost, slow carbonization and environmental problems associated high carbon footprints and solvent usage during the acrylonitrile, PAN and fiber (solution spinning) production.<sup>1</sup> Lignin can be considered as a “green” alternative for carbon fiber production.<sup>4</sup> Lignin along with hemicellulose and cellulose is one of the most abundant components of lignocellulosic biomass. Lignin is amorphous and the only aromatic biopolymer present in the cell walls of pith, roots, fruit, buds and bark. Lignin is synthesized by a dehydrogenative polymerisation of hydroxyl cinnamyl alcohol monomers called monolignols (p-coumaryl, coniferyl and sinapyl alcohol).<sup>5-6</sup> The vast majority of technical lignin is obtained from the paper and pulp industry where it is essentially a by-product used in low value energy applications. Lignin can be classified according to the industrial pulping processes used for its isolation (kraft, sulfite, soda and organosolv).<sup>2, 7-8</sup> These processes require high temperatures, high pressures and extreme pH, and therefore it produces alterations in the molecular structure of native lignin. Additionally, the differences between processing conditions of these isolation methods infer variations in terms of molecular weight and glass transition temperatures in the resulting lignins.<sup>2, 7-8</sup>

It is well known that lignin displays processing limitations such as a lack of melting and brittleness making industrial scalability challenging as carbon fibers need to be first processed into a precursor fiber via solution or melt extrusion and subsequently carbonized to carbon fiber. Melt extrusion is the favored route as it is less onerous on the environment and allows for the elimination of the use of toxic solvents during processing.<sup>4</sup> To allow lignin melt processing, chemical modification is required to infer thermoplastic behaviour and to increase ductility.<sup>9</sup> Several approaches have been described in an effort to improve the processability of this abundant raw material, for example, modifications to improve its thermoplastic behavior<sup>10</sup> and lignin blending with polymers.<sup>9, 11-17</sup> In terms of chemical modification, esterification and etherification are the most promising approaches to modify lignin, and acetylation is a routine method used to enhance the solubility of lignin samples for molecular weight assessment and structural analysis.<sup>18</sup> As alternative to chemical modification, lignin/polymer blending offers great potential as a processing aid in carbon fiber production however compatibility is of utmost importance. For example, poly(ethylene oxide) (PEO)<sup>9, 11-14</sup>, polyethylene terephthalate (PET)<sup>12-13</sup> and poly(N vinyl pyrrolidone) (PVP) have been found to be compatible. Polymers such as polylactic acid (PLA)<sup>16</sup> and polypropylene found to be incompatible.<sup>17</sup> During carbon fiber production incompatible blends generate porous structures after carbonization, and therefore are unsuitable for structural applications. Up to now, researchers have produced lignin and lignin blends which are capable of producing precursor fibers via melt processing.<sup>12, 14</sup> However, these precursor fibers remain brittle and unsuitable for the production of carbon fiber at scale and for structural applications.

In this context, we propose a segmented thermoplastic elastomeric polyurethanes as potential candidate for lignin blending. As the soft segment can be synthesized in a wide range of molecular functionalities, that can be compatible with lignin such as: polyester polyols and polyether polyols.<sup>19</sup> In addition, thermoplastic elastomeric polyurethanes can reduce lignin brittleness and increase flexibility allowing ease of processing. Also, the use of bio-based polyurethane for carbon fiber precursor will reduce the environmental impact and therefore increase the sustainability associated with carbon fiber production.

## **Experimental**

### *Materials*

Lignins: Alcell organosolv hardwood lignin (TcA) with a  $M_w$  of 4000 g/mol and hydroxypropyl modified Kraft hardwood (TcC) with a  $M_w$  of 11400 g/mol were obtained from Tecnar GmbH. (Germany). Thermoplastic polyurethane (TPU) Pearlthane ECO 12T95 was obtained from Veltex (France) (manufactured by Lubrizol) and it was synthesized from castor oil, methylene diphenyl diisocyanate and 1,4-butanediol, according to manufacture information. Dimethylacetamide (DMAc), LiBr and PMMA were purchased from Sigma Aldrich (Germany).

### *Fiber preparation*

Samples were extruded twice using an xplore MC15 microcompounder. Materials were compounded during the first run and the second run was used to produce precursor fibers. The spinneret diameter was 1.5 mm for compounding and 0.5 mm for spinning. All prepared samples and the temperature profile used are summarized in Table 1. The screw speed was 100 rpm for compounding and 50 rpm for fiber spinning.

### *Carbonization.*

Prior to carbonization the fibers were stabilized in air at a ramp of 0.1 °C/min from room temperature until 250 °C, with an isothermal treatment at 250 °C for one hour. Samples were carbonized in a quartz tube in nitrogen atmosphere at 1000 °C for 30 minutes using a heating rate of 10 °C/min. Carbonization of the samples for WAXS measurements was conducted at 1400 °C with a heating rate of 10 °C/min to be able to compare with PAN fibers (Toray T300).

**Table 1.** Composition, spinnability, and processing temperature profile for Lignin/TPU blends.

<b>TcA</b>				
<b>Sample name</b>	<b>Lignin content (%)</b>	<b>TPU content (%)</b>	<b>Processing temperature (°C)</b>	<b>Spinnability</b>
TcA/TPU_90/10	90	10	155/180/190/180	x
TcA/TPU_85/15	85	15	155/180/190/180	x
TcA/TPU_80/20	80	20	155/180/190/180	x
TcA/TPU_75/25	75	25	155/180/190/180	x
TcA/TPU_70/30	70	30	155/180/190/180	✓
TcA/TPU_65/35	65	35	155/180/190/180	✓
TcA/TPU_60/40	60	40	155/180/190/180	✓
TcA/TPU_55/45	55	45	155/180/190/180	✓
TcA/TPU_50/50	50	50	155/180/190/180	✓

<b>TcC</b>				
<b>Sample name</b>	<b>Lignin content (%)</b>	<b>TPU content (%)</b>	<b>Processing temperature (°C)</b>	<b>Spinnability</b>
TcC/TPU_90/10	90	10	175/190/200/190	x
TcC/TPU_85/15	85	15	175/190/200/190	x
TcC/TPU_80/20	80	20	175/190/200/190	x
TcC/TPU_75/25	75	25	175/190/200/190	x
TcC/TPU_70/30	70	30	175/190/200/190	✓
TcC/TPU_65/35	65	35	175/190/200/190	✓
TcC/TPU_60/40	60	40	175/190/200/190	✓
TcC/TPU_55/45	55	45	175/190/200/190	✓
TcC/TPU_50/50	50	50	175/190/200/190	✓

### *Characterization*

Size-exclusion chromatography (SEC) was performed on an Agilent 1260 infinity GPC system with refractive index detector. As stationary phase, a PolarSil linear S column from PSS Polymer Mainz was chosen while the mobile phase was dimethylacetamide (DMAc) with the addition of LiBr (5 g/l) according to the method of Clauss et. al.<sup>20</sup> Measurements were conducted at 50 °C and 0.75 ml/min and evaluated by conventional calibration against PMMA.

DSC analysis of the TPU blends was performed in a DSC 6 Perkin Elmer (USA). A first scan was done in order to delete the thermal history of the samples from room temperature to 120 °C using a heating rate of 20 °C/min under nitrogen atmosphere. The second scan, which was used for characterization, was carried out from room temperature to 250 °C using the same heating rate and atmosphere. Further thermal analysis was performed on a Netzsch STA 449F3 Jupiter equipped with a QMS 403C Aëolos mass spectrometer. Measurements were conducted under nitrogen at a heating rate of 10 K/min.

Fourier transform infrared spectroscopy (FTIR) measurements were performed using a Nicolet Nexus FTIR spectrometer over the range 450–4000  $\text{cm}^{-1}$  equipped with an attenuated total reflectance accessory (ATR), a total of 60 scans with a spectral resolution of 2  $\text{cm}^{-1}$  were recorded. Scanning Electron Microscopy (SEM) was performed to determine the blend morphology utilizing a Hitachi SU70 microscope at an accelerating voltage of 20 kV and a working distance of 14 mm. The fibers were placed in a sample holder (ca 2 cm diameter) to study the sample surface. For cross-section observation the samples were cryoscopically fractured. Rheological analysis was performed utilizing a

Discovery Hybrid Rheometer HR2 equipped with environmental test chamber from TA instruments. The samples were measured using a temperature ramp mode of 5 °C/min from 170 °C to 230 °C between 25.0 mm aluminium parallel plates at 1% strain and an angular frequency of 1 rad/s. Tensile properties of the precursor fibers were measured according to the ASTM 3379-75. The measurements were carried out in a DMA Q800 from TA instruments in tension mode at 25 °C at 1mm/min until 200 % strain. For the mechanical test of the carbonized samples, the fibers with 40 and 50 % of TPU were selected. These fibers were produced using a spinneret with diameter of 0.25 mm. Tensile properties were measured according to the ASTM 3379-75 in a Tinius Olsen H25KS tensile test machine using an average of 20 fibers per sample.

Wide-angle X-ray studies (WAXS) were conducted on an D/Max Rapid II from Rigaku at 40 kV and 30 mA with Cu-K(alpha)-radiation  $\lambda=0.15418$  nm. Diffraction patterns were recorded on a 0.8 collimator, with an oscillation of the samples between 20 and 30 ° and an imaging plate detector. The scan rate was 0.2 °/min with an interval of 0.045 °. The interlayer distance  $d_{002}$  was calculated using the position of the 002-reflection and Bragg's equation. The crystallite thickness  $L_c$  was determined with the (002) reflection and Scherrer's equation while the crystallite length  $L_a$  was determined using the (10) reflection and Scherrer's equation.

$$L_c = \frac{K\lambda}{\beta \cos\theta} \quad (1)$$

$K$  is the Scherrer form factor, for  $L_c$ ,  $K = 0.9$ . In case of  $L_a$ , the Scherrer form factor  $K = 1.83$ <sup>21</sup>.  $\beta$  is the full width at half maximum of the corresponding reflection.  $N_c$ , the average number of graphene layers in one crystallite, was determined by forming the quotient

$L_c/d_{002}$ . Curve fitting was done using PDXL software from Rigaku and split pseudo Voigt-type curves.

## Results and discussion

The difference in the molecular weight between both lignins is mainly attributed to the chemical modification carried out on the modified Kraft lignin by the reaction of lignin with propylene oxide. Both the Alcell and the modified lignin were processable from compounding to spinning in a wide range of TPU blending ratios. However, only samples with greater than 30 % of TPU were sufficiently ductile to withstand the automatic fiber winding process for extended periods of time in order to produce spools as shown in Figure S3. The increased ductility is attributed to the addition of the linear soft segment containing TPU.

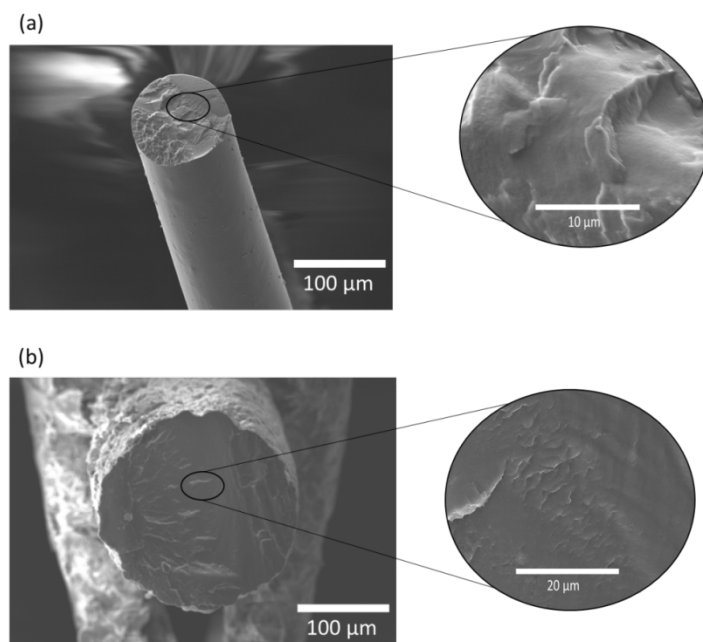


**Figure 1.** SEM images of the cross section of (a) Fb-TcA/TPU\_50/50 and (b) Fb-TcC/TPU\_50/50.



Figure 1 shows the SEM images of cross sections of the precursor fibers of TcA/TPU (Figure 2(a)) and TcC/TPU (Figure 2(b)). Again, in both cases the SEM analysis shows good compatibility of the blends, with no phase separation observed. These results confirm that the molecular interactions between lignin and TPU polymer chains create thermodynamically stable polymer blends preventing phase separation during the spinning process. The favorable blend compatibility is attributed to a) semipolar polyester groups in the soft segments of the TPU and b) the aromatic nature of the hard segment of TPU, allowing aromatic interactions such as  $\pi$ - $\pi$  stacking, and when this is combined with hydrogen bonding miscibility is increase<sup>22-24</sup>.

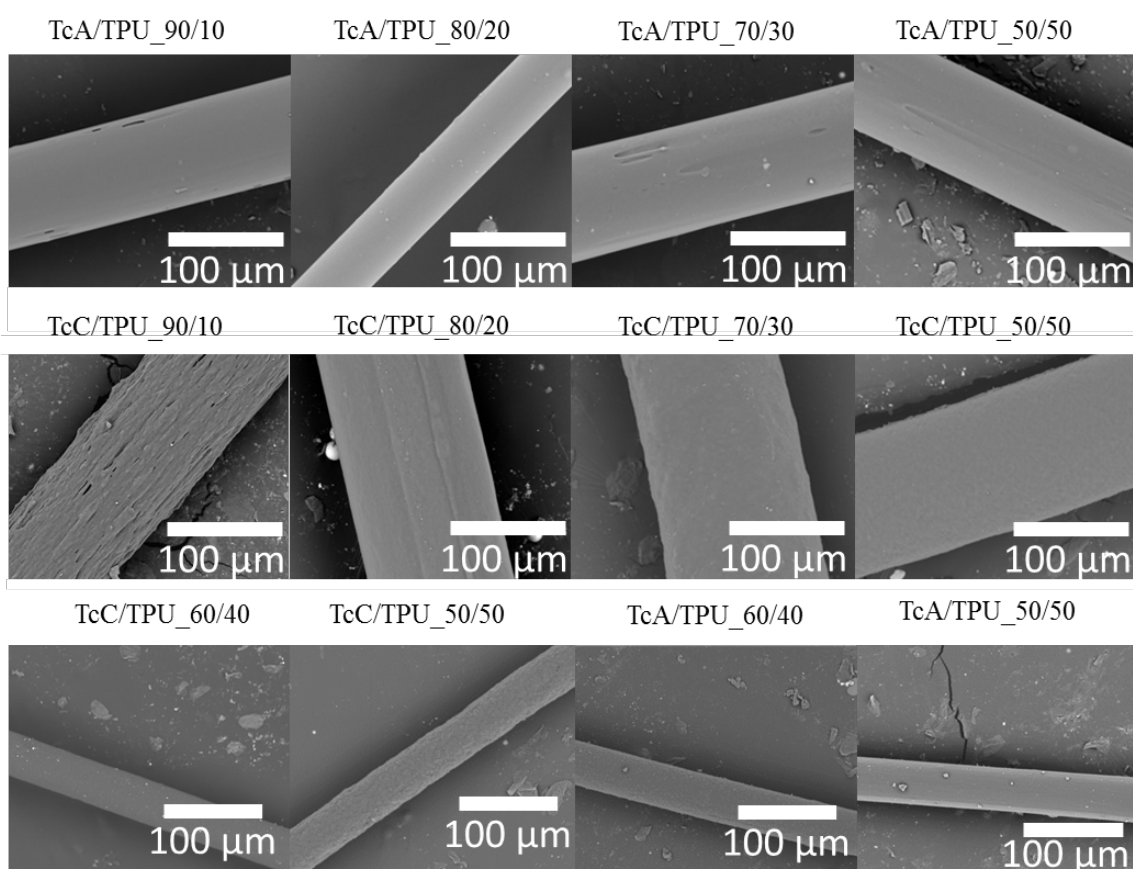


**Figure 2.** SEM images of precursor fibers based on lignin/TPU blends. First and second rows fibers produced using 0.5 mm die and third row fibers produced using 0.25 mm

Figure 2 shows SEM images of the precursor fiber surfaces. For the case of TcA/TPU blends a smooth surface was obtained indicating a good mixing and compatibility between both components. However, for the fiber composed by TcC/TPU certain degree of roughness is observed, that decreases when the TPU content increases, as shown in Figure 3. It is obvious that the blend morphology depends on the molecular interactions between these two polymers. For this reason, the structural and chemical differences between TcC and TcA play an important role in the final morphology of Lignin/TPU blends. The size of the precursor fibers is in the range of 70-150  $\mu\text{m}$  diameters, these can be reduced using smaller dies (250  $\mu\text{m}$ ) and with stretching during the fiber winding process making it possible to obtain precursor fibers with a diameter around 50  $\mu\text{m}$  (see third row of Figure 2).

The chemical structure of the TcA/TPU and TcC/TPU blends was analyzed using Fourier Transformed Infrared spectroscopy (FTIR) in the ATR mode. Figure 4 shows the spectra for the two blends at different compositions and Table S2 and S3 show the assignments for the FTIR resonance bands of the lignins<sup>25-26</sup> and of TPU.<sup>27-28</sup> All compositions with high lignin content show its characteristic signal. The blends from 65% lignin and below show signals characteristic of TPU in the form of a shoulder at 1530  $\text{cm}^{-1}$ , for the OCN stretching vibration.

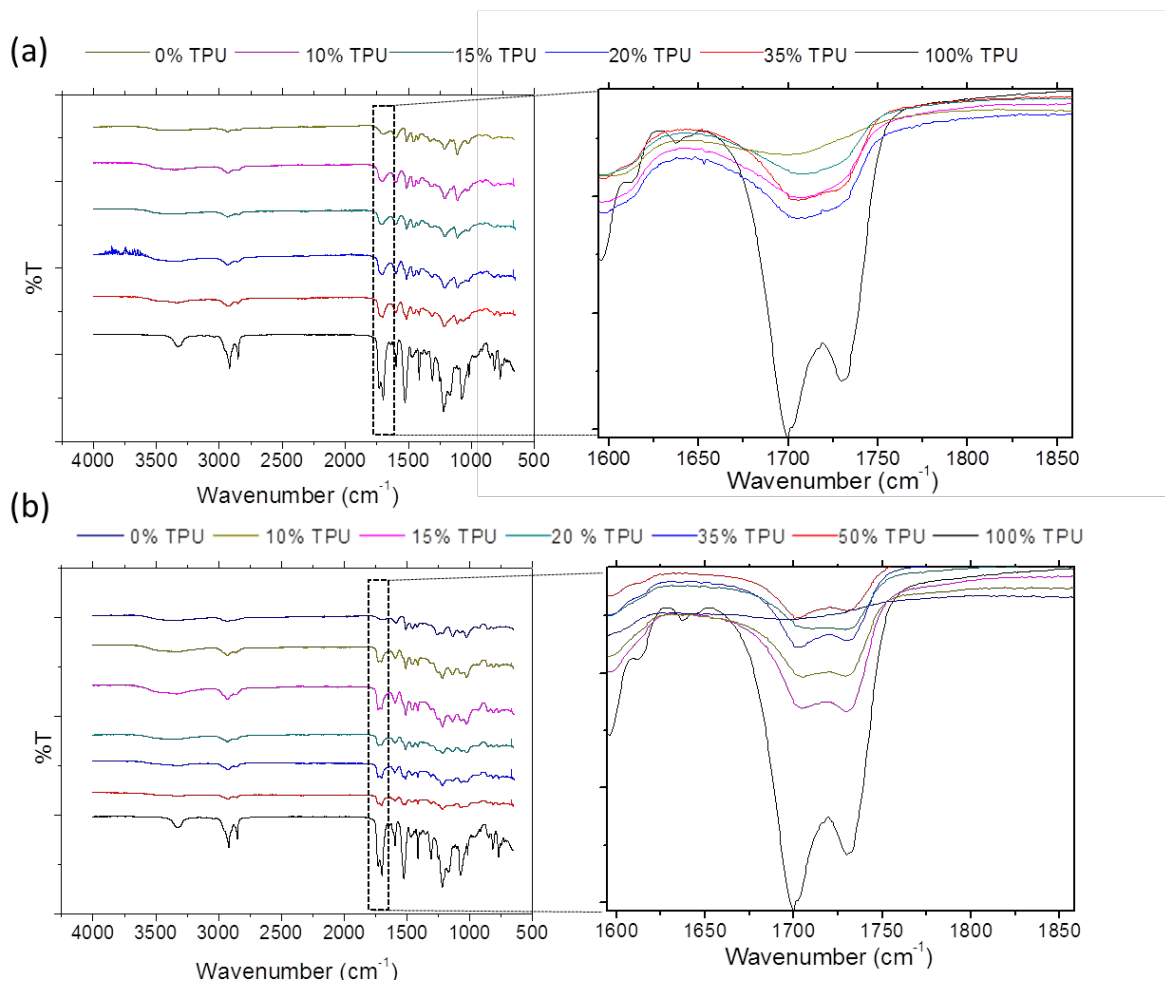


**Figure 3.** FTIR spectra of (a) TcA/TPU and (b) TcC/TPU blends as a function of the TPU content with an inset in the carbonyl vibration region.

TPU shows the typical band for C=O stretching located at 1700 and 1740  $\text{cm}^{-1}$ . The band centered at 1700  $\text{cm}^{-1}$  is assigned to the H- bonded carbonyl groups while the vibration centered at 1740  $\text{cm}^{-1}$  correspond to free C=O.<sup>27-28</sup> The insets of the Figures 3 (a) and (b) show obvious difference in the carbonyl band indicating that the two lignins exhibit a different degree of H- bonding interactions with TPU. The carbonyl signal of the blends is slightly shifted compared to the raw materials indicating strong interaction between both lignins and TPU.

For the case of TcA only a local maximum is observed centered at  $1707\text{ cm}^{-1}$ , indicating that the number of H-bonded C=O groups increases compared to the free carbonyl groups. Thus, TcA is favorable for H-bond interactions with TPU. However for the case of TcC the opposite trend is observed. TcC exhibit two local maximums at  $1704\text{ cm}^{-1}$  and  $1730\text{ cm}^{-1}$ . The results indicate that number of free C=O groups increases with the addition of TcC. This indicates that the presence of lignin TcC inhibits the formation of Hydrogen bonding between TPU molecules since the TcC polymer chains are interacting via Van der Waals forces.

Figure 4 shows the DSC curves of the Lignin/TPU blends. The same trend is observed in both lignins, the melting point of TPU ( $183\text{ }^{\circ}\text{C}$ ) decreases with the presence of lignin. However, the  $T_g$  of the samples based on TcA was not observed when the TPU was higher than 35 % in the temperature range from 40 to  $250\text{ }^{\circ}\text{C}$ . This fact can be explained as the chemical interaction between the soft segment of TPU and lignin polymer chains begins. As consequence of those interactions the temperature of  $T_g$  decreases below room temperature as TPU acts as a lignin plasticizer. In contrast, the blends based on TcC showed an increase of the  $T_g$  from  $112$  to  $126\text{ }^{\circ}\text{C}$  with addition of TPU due to the presence of TPU chains that reduce the movement of lignin chains. This is attributed to the structural differences between TcC and TcA generated by the hydroxypropyl modification of TcC.

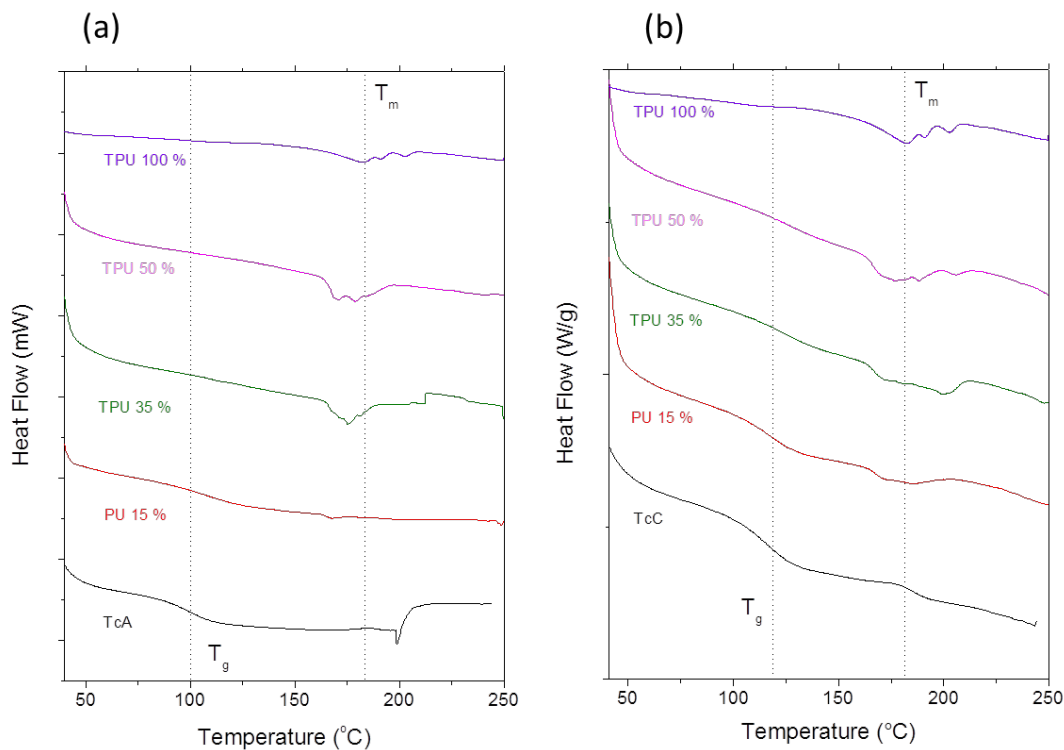


**Figure 4.** DSC curves of (a) TcA/TPU and (b) TcC/TPU blends as a function of the TPU content.

DSC parameters such as: glass transition and melting temperature are summarized in the Table S4.

Rheological analysis was carried out to determine the viscoelastic behavior of the carbon fiber precursor. Figure 6 shows the complex viscosity as a function of temperature for the samples based on the Alcell lignin (Figure 5 (a)) and the hydroxypropyl modified lignin (Figure 5(b)). For the case of the polymer blends based on Alcell lignin the viscosity decreases with the temperature between 190-200 °C however, for the blends with a TPU content higher than 35 % the viscosity increases from 210 °C due to the crosslinking reactions between lignin chains.<sup>29</sup>

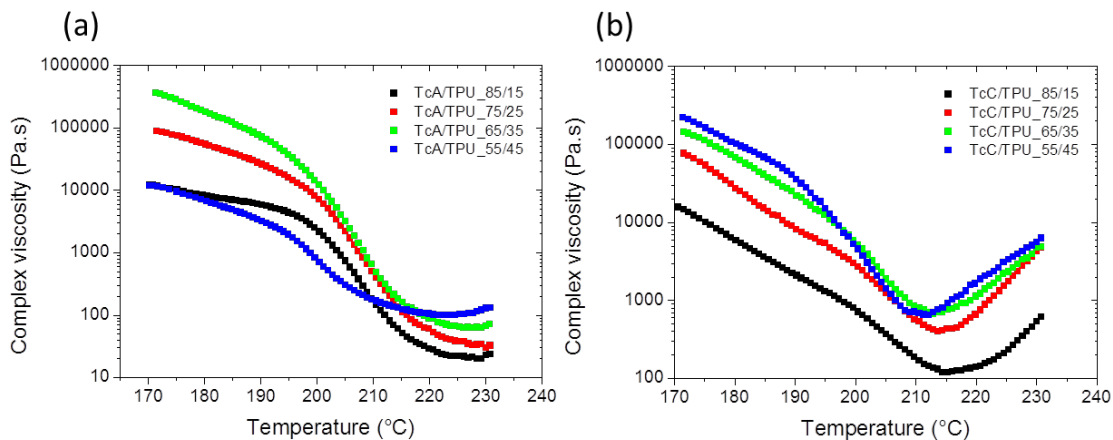


**Figure 5.** Viscosity as a function of temperature for lignin/TPU blends based on (a) Alcell lignin (TcA) and (b) hydroxypropyl modified lignin (TcC).

For the case of the blends based on hydroxypropyl lignin the viscosity decreases until 217 °C for the samples with 15 % of TPU, 214 °C for a 25 % of TPU content, 212 °C for the blends with 35 % of TPU and 210 °C for the samples composed of 45 % of TPU. After those temperature values the viscosity increases mainly dominated by the crosslinking reactions between lignin molecules. However, this effect is augmented as the TPU content increases. This fact, suggests strong interactions between the cross-linked polymer chains of lignin and TPU.

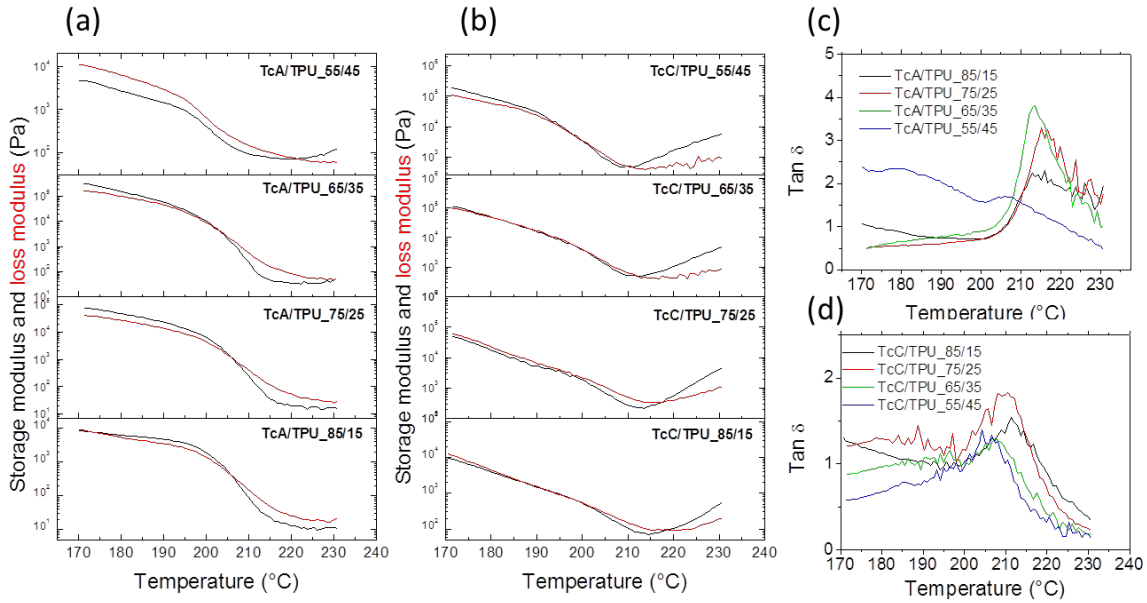


**Figure 6.** Storage and loss modulus as a function of temperature for lignin/TPU blends based on (a) TcA and (b) TcC. Tan delta of lignin/TPU blends based on (c) TcA and (d) TcC.

The  $G'$  of all the samples decreased as a function of the temperature between 170-195 °C, then, drastically decreases from 195 to 220 °C as the TPU approached its melt temperature. Temperature dependency of the loss modulus ( $G''$ ) for all specimens is shown in Figure 6 (a) and (b). Similar trends were found for the  $G''$  results. The drastic reduction of both  $G'$  and  $G''$  from 200 to 230 °C was due to the transition from the rubbery plateau to viscous behavior. For the case of the TcA /TPU samples  $G''$  is higher than  $G'$  when the TPU content is 15 % at 170 °C indicating liquid-like behavior. However,  $G'$  increases at 180 °C which suggest that the interactions between both components begins inferring the onset of elastic behavior. At 205 °C the transition from elastic to viscos behavior is complete. Samples with a TPU content of 25 % and 35 % display the same trend. with the transition temperature being 203 °C for 35% and 205 °C for 25 % confirming the plasticization effect

of TPU on alcell lignin. For 45 % TPU content the  $G''$  is higher than  $G'$  until 221 °C, then the  $G'$  increases as a result of the crosslinking reaction between the lignin polymer chains.<sup>29</sup> For samples prepared using hydroxypropyl modified lignin,  $G'$  and  $G''$  curves show a different viscoelastic behavior compared to TcA samples due to the different nature of the interaction between both polymers. The samples with 15 % and 25 % of TPU, showed a liquid-like behavior since  $G''$  is higher than  $G'$  until 220 °C. However, when TPU content increases from 35 % to 45 % the transition from elastic to viscous behavior is observed at 200 °C. Then, in the temperature range of 210-212 °C  $G'$  increases again due to the crosslinking reactions of lignin.<sup>29</sup> It is possible to observe a clear relationship between this crossover temperature and the TPU content. The crossover temperature decreases as the TPU content increases. This fact suggests that the presence of TPU chains initiates the crosslinking reaction between TcC polymer chains.

The temperature dependency of the loss tangent,  $\tan \delta$ , for all specimens is shown in Figure 6 (c) and (d). All the blends show a peak in the range 200-220 °C that corresponds with the maximum degree of molecular movement of the polymers chains in the blend due to the liquid-like behavior obtaining the minimum viscosity values in this temperature range. Thus, the temperature profile chosen for precursor fiber processing is the optimum since the flow behavior is ideal in terms of viscosity and there are no crosslinking reactions occurring in this temperature range.



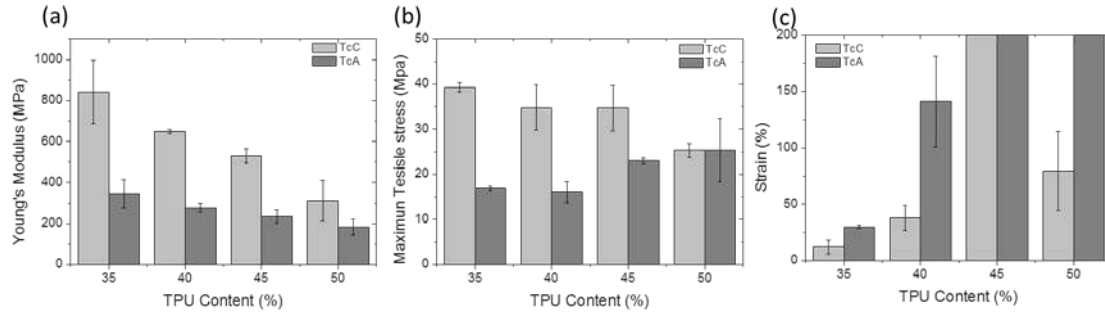


**Figure 7.** Mechanical properties of Lignin/TPU precursor fibers.

Mechanical properties obtained from the stress-strain curves of single fibers are shown in Figure 7. Precursor fibers with a TPU content below 35 wt.-% were too brittle to be measured. The addition of TPU produced a drastic increase in mechanical performance in both lignins. Obviously, the different nature of the interactions between each Lignin and TPU causes differences in the observed mechanical response. Alcell and hydroxypropyl modified lignin both showed an increase in their Young's moduli (Figure 7(a)) values being higher for the fibers based on hydroxypropyl modified lignin. However, the behavior in terms of maximum tensile stress is the opposite. At 50 % of TPU content both lignin show the same value for maximum tensile stress, around 25 MPa, indicating that TPU is the dominant factor in the blend in terms of the tensile performance. . However, at lower TPU content the maximum tensile stress decreases to 17 MPa for Alcell while it increases to 39 MPa for hydroxypropyl modified lignin. In addition, some differences were observed in the strain behavior (Figure 7 (c)). The results confirm that the addition of TPU produces a plasticizing effect over both lignins as the plastic deformation increases with TPU content. Alcell /TPU precursor fibers showed higher values of deformation compared to hydroxypropyl modified lignin/TPU samples. However, the elongation decreases for both blends with 40 and 35 % TPU due to the brittleness of both lignins.

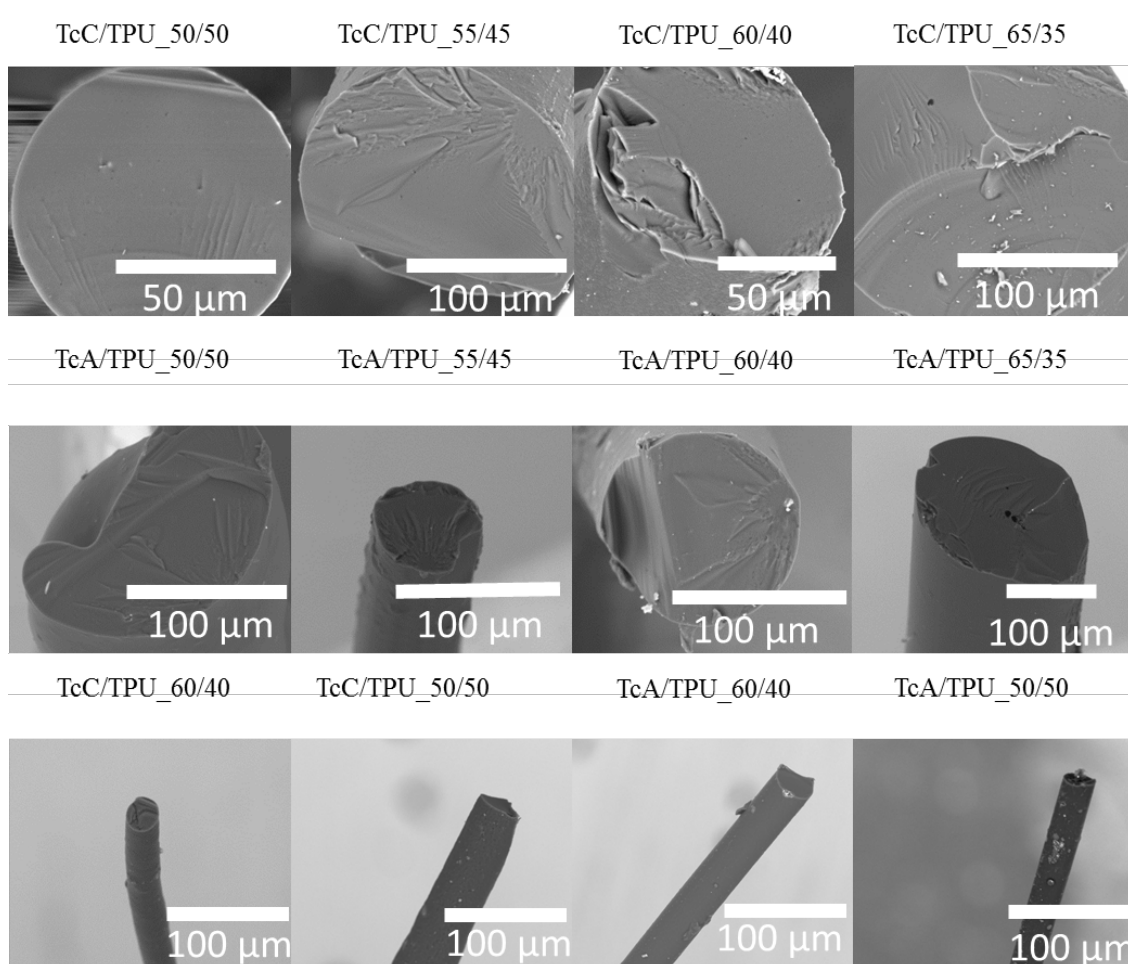


**Figure 8.** SEM images of precursor fibers based on lignin/TPU blends. First and second rows fibers produced using 0.5 mm spinneret and third row fibers produced using 0.25 mm

Figure 8 shows the cross section of the precursor fibers after they have been carbonized to carbon fiber. The images clearly display a smooth homogeneous morphology with absence of detrimental porosity. The diameters of the fibers after carbonization were in the range 70-150  $\mu\text{m}$  and between 23-32  $\mu\text{m}$  for the fibers produced with spinneret diameter of 500 and 250  $\mu\text{m}$  respectively.

Thermo-gravimetric analysis is an effective method to analyze the precursor fiber during the thermal conversion to carbon fiber. It is of utmost importance to produce a carbon fiber

which is compact and defect-free. Therefore, a high carbon yield of the precursor is essential. It is well known that for PAN-based carbon fibers, a high carbon yield, which is directly related to a low porosity and high density of the fiber, translates into good mechanical properties of the CF<sup>30-31</sup>. Our results (see Figure 9 and Table 2) show that, carbon yields vary between 26 and 36 weight percent at 1400 °C. Despite different molar mass and thermal properties, carbon yield of Alcell and hydroxypropyl modified lignin blends differ very little. Interestingly, modified and untreated Alcell lignin shows a residual mass of 34.75 and 38.5 wt.-percent at 1400 °C respectively. Its early mass loss and low carbon yield is attributed to the evaporation of low molar mass fractions. Compared to our blend fibers, we were able to almost reach 37 % yield with the addition of TPU. We assume the higher yield of our blends is also attributed to the extrusion processing step which may induce condensation reactions and the loss of volatile matter.

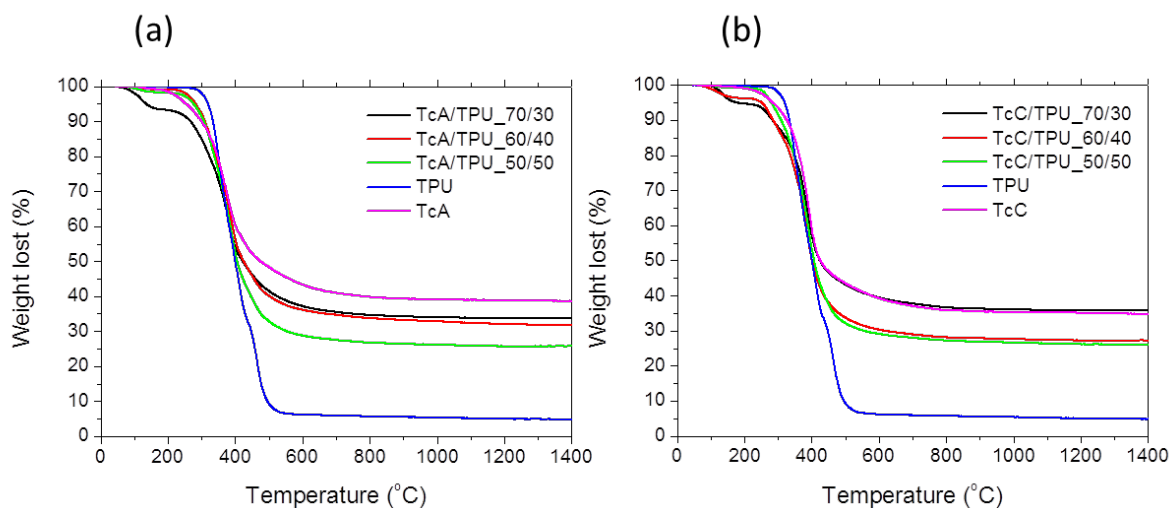


**Figure 9.** TGA measurements of lignin/TPU blends under nitrogen and a heating rate of 10 C/min.

**Table 2.** Carbon yields of lignin/TPU blends determined by TGA under nitrogen.

TPU content [wt.- %]	Carbon yield blended with TcA	Carbon yield blended with TcC
	[%]	[%]
100	4.80	4.80
50	25.76	26.07
40	31.73	28.61
30	33.67	35.84
0	38.50	34.75

The carbonized fibers were investigated using wide angle x-ray scattering (WAXS). Structural parameters such as carbon crystallite dimension and the interlayer distance as well as the orientation of the crystallites were determined.

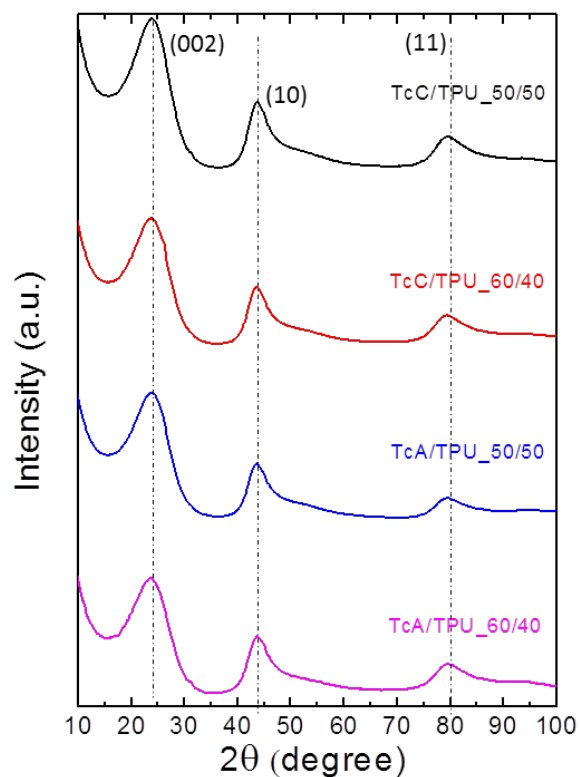


**Figure 10.** X-ray diffraction spectra of Lignin/TPU carbon fibers.

Figure 10 shows the X-ray diffraction spectra of Lignin/TPU carbon fibers (1400 °C) with the typical reflections of graphitic structures near 24, 44 and 79 ° 2 $\theta$  that correspond to the reflection planes (002), (10) and (11) respectively. Perfect graphite exhibits the (002) reflection at 26.5° and accordingly a  $d_{002}$  of 0.3354 nm. In carbon fibers, this value is generally not reached because they also contain amorphous and turbostratic carbon.<sup>32</sup> The crystallite sizes  $L_c$  and  $L_a$  determined by equation (1) are shown in Table 3.

**Table 3.** Peak position,  $d_{002}$ -spacing and crystallite sizes (L) of Lignin/TPU carbon fibers

Sample	(002) [°]	$d_{002}$ [nm]	$L_a$ (10) [nm]	$L_c$ [nm]
TcA-TPU 60-40	24.05	0.38	3.40	1.05
TcA-TPU 50-50	24.28	0.37	3.68	1.03
TcC-TPU 60-40	24.29	0.37	3.64	0.98
TcC-TPU 50-50	24.35	0.37	3.65	1.08
Toray T300	25.20	0.36	3.77	1.29

Of special interest is a comparison of the structural data of the lignin/TPU-based CF with those of a commercial PAN-based CF (Toray T300). While crystallite dimensions were similar the most significant difference was observed in the position of the (002) reflection and therefore  $d_{002}$ . Here, the lignin-based fiber showed slightly larger distance (0.359 vs. 0.37 – 0.38 nm at 1400°C).

**Table 4.** Mechanical properties of Lignin/TPU carbon fibers.

<b>Precursor fiber</b>	<b>Tensile strength (MPa)</b>	<b>Modulus (GPa)</b>	<b>Elongation (%)</b>	<b>Diameter (<math>\mu\text{m}</math>)</b>
TcA-TPU 60-40	660 $\pm$ 110	61 $\pm$ 7	1 $\pm$ 0.2	31 $\pm$ 2
TcA-TPU 50-50	1100 $\pm$ 100	80 $\pm$ 10	1.4 $\pm$ 0.3	25 $\pm$ 3
TcC-TPU 60-40	620 $\pm$ 90	60 $\pm$ 10	1.1 $\pm$ 0.2	31 $\pm$ 2
TcC-TPU 50-50	800 $\pm$ 100	66 $\pm$ 10	1.2 $\pm$ 0.2	30 $\pm$ 1

Mechanical properties of the carbon fibers are shown in Table 4. Generally, tensile strength and Young's modulus values of TPU/Lignin carbon fibers are higher compared to pure lignin<sup>12</sup> (605 MPa tensile stress and 60 GPa modulus). Very promising values of tensile strength have been obtained for the sample TcA-TPU 50-50 (1.1 GPa) which is higher than other reported blends of lignin such as: Lignin/PET (700 MPa), ratio 75:25<sup>12</sup>, or Lignin/polypropylene (437 MPa), ratio 87.5:12.5<sup>12</sup>. Compared to commercial PAN T300 fibers (3.45 tensile stress and 230 GPa modulus)<sup>33</sup> and E-Glass Fibers (1.8 tensile stress and 76 GPa modulus)<sup>34</sup> the values of Lignin /TPU fibers are lower. However, PAN fibers are produced in an industrial scale with a diameter around 5  $\mu\text{m}$  and is a mature optimized technology. Nevertheless, Lignin/TPU carbon fibers are showing real promise.

## Conclusions

Precursor fibers of a blend of lignin with thermoplastic polyurethane (TPU) were successfully prepared by continuous melt spinning and subsequently converted to carbon fibers. Alcell organosolv hardwood lignin and hydroxypropyl modified Kraft hardwood lignin showed excellent miscibility with TPU due to the absence of any phase separation in the observed concentration range during the spinning and carbonization process. The

differences in the molecular structure of each lignin caused differences in the degree of interaction with TPU, with H-bonding interactions more relevant in samples containing Alcell organosolv hardwood lignin. The optimum temperature range for melt spinning is between 200-210 °C since higher temperatures promote crosslinking reactions. The precursor material obtained good carbon yields, around 40 wt.-%, which are close to pure lignin indicating condensation reactions between both polymers. X-ray diffraction patterns showed similar structural properties of the lignin/TPU-based carbon fiber compared to a commercial PAN-based CF. In addition carbon fibres with high mechanical properties were obtained especially for the sample TcA-TPU 50-50 (1.1 GPa tensile stress with a modulus of 80 GPa modulus). Thus, the blend of bio-based thermoplastic elastomer polyurethane with lignin shows an enormous potential as precursor for carbon production and is a potential alternative to PAN as precursor material.

## ASSOCIATED CONTENT

### **Supporting Information.**

Additional information of: raw materials, FTIR, rheology, DSC and Images of precursor fibers

### **Acknowledgment**

The authors acknowledge received funding from the BioBased Industries Joint Undertaking under the European Union's Horizon 2020 research and innovation programme under grant agreement No 720707.

## Corresponding Author

\*Mario Culebras. Email: [mario.culebrasrubio@ul.ie](mailto:mario.culebrasrubio@ul.ie)

\*Maurice Collins. Email: [Maurice.collins@ul.ie](mailto:Maurice.collins@ul.ie)

## References

- (1) Mainka, H.; Täger, O.; Körner, E.; Hilfert, L.; Busse, S.; Edelmann, F. T.; Herrmann, A. S. Lignin – an alternative precursor for sustainable and cost-effective automotive carbon fiber. *Journal of Materials Research and Technology* **2015**, *4* (3), 283-296, DOI: 10.1016/j.jmrt.2015.03.004.
- (2) Fang, W.; Yang, S.; Wang, X.-L.; Yuan, T.-Q.; Sun, R.-C. Manufacture and application of lignin-based carbon fibers (LCFs) and lignin-based carbon nanofibers (LCNFs). *Green Chemistry* **2017**, *19* (8), 1794-1827, DOI: 10.1039/C6GC03206K.
- (3) Fitzer, E. Pan-based carbon fibers—present state and trend of the technology from the viewpoint of possibilities and limits to influence and to control the fiber properties by the process parameters. *Carbon* **1989**, *27* (5), 621-645, DOI: 10.1016/0008-6223(89)90197-8.
- (4) Frank, E.; Steudle, L. M.; Ingildeev, D.; Spörl, J. M.; Buchmeiser, M. R. Carbon fibers: precursor systems, processing, structure, and properties. *Angewandte Chemie International Edition* **2014**, *53* (21), 5262-5298, DOI: 10.1002/anie.201306129
- (5) Wang, C.; Kelley, S. S.; Venditti, R. A. Lignin-Based Thermoplastic Materials. *ChemSusChem* **2016**, *9* (8), 770-83, DOI: 10.1002/cssc.201501531.
- (6) Zhu, H.; Luo, W.; Ciesielski, P. N.; Fang, Z.; Zhu, J. Y.; Henriksson, G.; Himmel, M. E.; Hu, L. Wood-Derived Materials for Green Electronics, Biological Devices, and Energy Applications. *Chem Rev* **2016**, *116* (16), 9305-74, DOI: 10.1021/acs.chemrev.6b00225.
- (7) Gillet, S.; Aguedo, M.; Petitjean, L.; Morais, A. R. C.; da Costa Lopes, A. M.; Łukasik, R. M.; Anastas, P. T. Lignin transformations for high value applications: towards targeted modifications using green chemistry. *Green Chemistry* **2017**, *19* (18), 4200-4233, DOI: 10.1039/c7gc01479a.
- (8) Suhas; Carrott, P. J. M.; Ribeiro Carrott, M. M. L. Lignin – from natural adsorbent to activated carbon: A review. *Bioresource Technology* **2007**, *98* (12), 2301-2312, DOI: 10.1016/j.biortech.2006.08.008.
- (9) Kubo, S.; Kadla, J. F. Kraft lignin/poly(ethylene oxide) blends: Effect of lignin structure on miscibility and hydrogen bonding. *Journal of Applied Polymer Science* **2005**, *98* (3), 1437-1444, DOI: 10.1002/app.22245.
- (10) Laurichesse, S.; Avérous, L. Chemical modification of lignins: Towards biobased polymers. *Progress in Polymer Science* **2014**, *39* (7), 1266-1290, DOI: 10.1016/j.progpolymsci.2013.11.004.
- (11) Kubo, S.; Kadla, J. F. Poly(Ethylene Oxide)/Organosolv Lignin Blends: Relationship between Thermal Properties, Chemical Structure, and Blend Behavior. *Macromolecules* **2004**, *37* (18), 6904-6911, DOI: 10.1021/ma0490552.
- (12) Kubo, S.; Kadla, J. F. Lignin-based Carbon Fibers: Effect of Synthetic Polymer Blending on Fiber Properties. *Journal of Polymers and the Environment* **2005**, *13* (2), 97-105, DOI: 10.1007/s10924-005-2941-0.



- (13) Kadla, J. F.; Kubo, S. Lignin-based polymer blends: analysis of intermolecular interactions in lignin–synthetic polymer blends. *Composites Part A: Applied Science and Manufacturing* **2004**, *35* (3), 395-400, DOI: 10.1016/j.compositesa.2003.09.019.
- (14) Kadla, J. F.; Kubo, S.; Venditti, R. A.; Gilbert, R. D.; Compere, A. L.; Griffith, W. Lignin-based carbon fibers for composite fiber applications. *Carbon* **2002**, *40* (15), 2913-2920, DOI: 10.1016/S0008-6223(02)00248-8.
- (15) Teramoto, Y.; Lee, S.-H.; Endo, T. Molecular composite of lignin: Miscibility and complex formation of organosolv lignin and its acetates with synthetic polymers containing vinyl pyrrolidone and/or vinyl acetate units. *Journal of Applied Polymer Science* **2012**, *125* (3), 2063-2070, DOI: 10.1002/app.36294.
- (16) Thunga, M.; Chen, K.; Grewell, D.; Kessler, M. R. Bio-renewable precursor fibers from lignin/poly lactide blends for conversion to carbon fibers. *Carbon* **2014**, *68*, 159-166, DOI: 10.1016/j.carbon.2013.10.075.
- (17) Kadla, J. F.; Kubo, S.; Venditti, R. A.; Gilbert, R. D. Novel hollow core fibers prepared from lignin polypropylene blends. *Journal of Applied Polymer Science* **2002**, *85* (6), 1353-1355, DOI: 10.1002/app.10640.
- (18) Zhang, M.; Ogale, A. A. Carbon fibers from dry-spinning of acetylated softwood kraft lignin. *Carbon* **2014**, *69*, 626-629, DOI: 10.1016/j.carbon.2013.12.015.
- (19) Ciobanu, C.; Ungureanu, M.; Ignat, L.; Ungureanu, D.; Popa, V. I. Properties of lignin–polyurethane films prepared by casting method. *Industrial Crops and Products* **2004**, *20* (2), 231-241, DOI: 10.1016/j.indcrop.2004.04.024.
- (20) Clauss, M. M.; Weldin, D. L.; Frank, E.; Giebel, E.; Buchmeiser, M. R. Size-Exclusion Chromatography and Aggregation Studies of Acetylated Lignins in N,N-Dimethylacetamide in the Presence of Salts. *Macromolecular Chemistry and Physics* **2015**, *216* (20), 2012-2019, DOI: 10.1002/macp.201500222.
- (21) Warren, B. E.; Bodenstern, P. The shape of two-dimensional carbon black reflections. *Acta Crystallographica* **1966**, *20* (5), 602-605, DOI: doi:10.1107/S0365110X66001464.
- (22) Szabó, G.; Romhányi, V.; Kun, D.; Renner, K.; Pukánszky, B. Competitive Interactions in Aromatic Polymer/Lignosulfonate Blends. *ACS Sustainable Chemistry & Engineering* **2016**, *5* (1), 410-419, DOI: 10.1021/acssuschemeng.6b01785.
- (23) Chen, R.; Abdelwahab, M. A.; Misra, M.; Mohanty, A. K. Biobased Ternary Blends of Lignin, Poly(Lactic Acid), and Poly(Butylene Adipate-co-Terephthalate): The Effect of Lignin Heterogeneity on Blend Morphology and Compatibility. *Journal of Polymers and the Environment* **2014**, *22* (4), 439-448, DOI: 10.1007/s10924-014-0704-5.
- (24) Bahl, K.; Swanson, N.; Pugh, C.; Jana, S. C. Polybutadiene- g -poly(pentafluorostyrene) as a coupling agent for lignin-filled rubber compounds. *Polymer* **2014**, *55* (26), 6754-6763, DOI: 10.1016/j.polymer.2014.11.008.
- (25) Boeriu, C. G.; Bravo, D.; Gosselink, R. J. A.; van Dam, J. E. G. Characterisation of structure-dependent functional properties of lignin with infrared spectroscopy. *Industrial Crops and Products* **2004**, *20* (2), 205-218, DOI: 10.1016/j.indcrop.2004.04.022.
- (26) Faix, O. Classification of lignins from different botanical origins by FT-IR spectroscopy. *Holzforchung-International Journal of the Biology, Chemistry, Physics and Technology of Wood* **1991**, *45* (s1), 21-28.
- (27) Yen, F.-S.; Lin, L.-L.; Hong, J.-L. Hydrogen-Bond Interactions between Urethane–Urethane and Urethane–Ester Linkages in a Liquid Crystalline Poly(ester–urethane). *Macromolecules* **1999**, *32* (9), 3068-3079, DOI: 10.1021/ma9804186.

- (28) Senich, G. A.; MacKnight, W. J. Fourier Transform Infrared Thermal Analysis of a Segmented Polyurethane. *Macromolecules* **1980**, *13* (1), 106-110, DOI: 10.1021/ma60073a021.
- (29) Sun, Q.; Khunsupat, R.; Akato, K.; Tao, J.; Labbé, N.; Gallego, N. C.; Bozell, J. J.; Rials, T. G.; Tuskan, G. A.; Tschaplinski, T. J. A study of poplar organosolv lignin after melt rheology treatment as carbon fiber precursors. *Green Chemistry* **2016**, *18* (18), 5015-5024, DOI: 10.1039/C6GC00977H.
- (30) Mittal, J.; Bahl, O.; Mathur, R. Single step carbonization and graphitization of highly stabilized PAN fibers. *Carbon* **1997**, *35* (8), 1196-1197, DOI: 10.1016/S0008-6223(97)84653-2.
- (31) Qin, X.; Lu, Y.; Xiao, H.; Zhao, W. Effect of heating and stretching polyacrylonitrile precursor fibers in steam on the properties of stabilized fibers and carbon fibers. *Polymer Engineering & Science* **2013**, *53* (4), 827-832, DOI: 10.1002/pen.23328.
- (32) Takaku, A.; Shioya, M. X-ray measurements and the structure of polyacrylonitrile-and pitch-based carbon fibres. *Journal of Materials Science* **1990**, *25* (11), 4873-4879, DOI: 10.1007/BF01129955.
- (33) Wang, S.; Chen, Z.-H.; Ma, W.-J.; Ma, Q.-S. Influence of heat treatment on physical-chemical properties of PAN-based carbon fiber. *Ceramics International* **2006**, *32* (3), 291-295, DOI: 10.1016/j.ceramint.2005.02.014.
- (34) Fiore, V.; Scalici, T.; Di Bella, G.; Valenza, A. A review on basalt fibre and its composites. *Composites Part B: Engineering* **2015**, *74*, 74-94, DOI: 10.1016/j.compositesb.2014.12.034.

## Table of Contents Graphic and Synopsis



Biopolymer blends based on lignin are a “green” alternative to petroleum based carbon fiber precursors, increasing the sustainability associated with carbon fiber production.